Pore formation in fluctuating membranes

Oded Farago
Materials Research Laboratory, University of California, Santa Barbara, California 93106 and Department of Physics, Korea Advanced Institute of Science and Technology (KAIST), 373-1 Kusong-dong, Yusong-gu, Taejon 305-701, South Korea

Christian D. Santangelo[a)]
Physics Department, University of California, Santa Barbara, California 93106

(Received 7 September 2004; accepted 28 October 2004; published online 4 January 2005)

We study the nucleation of a single pore in a fluctuating lipid membrane, specifically taking into account the membrane fluctuations, as well as the shape fluctuations of the pore. For large enough pores, the nucleation free energy is well-described by shifts in the effective membrane surface tension and the pore line tension. Using our framework, we derive the stability criteria for the various pore formation regimes. In addition to the well-known large-tension regime from the classical nucleation theory of pores, we also find a low-tension regime in which the effective line and surface tensions can change sign from their bare values. The latter scenario takes place at sufficiently high temperatures, where the opening of a stable pore of finite size is entropically favorable. © *2005 American Institute of Physics.* [DOI: 10.1063/1.1835952]

I. INTRODUCTION

Lipid bilayers play an important role in living cells as barriers separating the inside of the cell from the extracellular environment, as well as segregating the cell into separate internal compartments.[1] A vital feature of those membranes is the ability to remain intact under variety of external perturbations.[2] At the same time, however, many cellular processes, including endo- and exocytosis, lysis, and cell signaling require breaking the membrane structure and forming a nonbilayer transient, such as a membrane pore.[3–6] The opening of stable pores in biological membranes is also an important step for drug delivery[7] and gene therapy.[8] Consequently, much attention has been focused on understanding the processes leading to the formation of pores and the mechanisms controlling their stability.

Two types of pores dominate membrane permeability: free lipid pores and peptide-lined pores.[9] The interest in lipid pores has greatly increased in the past few years with the development of new experimental techniques to induce and study pore formation in biomimetic, single-component, lipid membranes. One approach to nucleate a pore is known as electroporation, where an electric field that produces compressive stress is used to disrupt the membrane.[10–14] Holes in lipid membranes have also been opened by other methods, including intense illumination,[15,16] suction through a micropipette,[17] adhesion on porous or decorated substrates,[18,19] and osmotic swelling.[20,21]

Most theories of pore formation to date derive from a model based on classical nucleation theory.[22] The model conceives the membrane as a two dimensional elastic medium characterized by a free energy per unit area (''surface tension'') σ. The formation of a circular hole of radius r_0 is driven by the reduction in the tension energy $-\sigma\pi r_0^2$ and is opposed by an edge energy proportional the pore perimeter $\Gamma 2\pi r_0$, where Γ, the line tension, denotes the energy per unit length along the pore's rim. The net energy is, thus, given by

$$E=\Gamma 2\pi r_0-\sigma\pi r_0^2. \tag{1}$$

Assuming $\Gamma>0$ and $\sigma>0$, Eq. (1) predicts that a pore with a radius larger than the critical value of

$$r_0>\frac{\Gamma}{\sigma} \tag{2}$$

is unstable in the sense that it will grow without bound and, ultimately, will rupture the membrane. Such a large pore will be created only if the nucleation energy barrier

$$\delta E=\frac{\pi\Gamma^2}{\sigma} \tag{3}$$

is accessible by thermal fluctuations. For typical estimates of the line tension, $\Gamma\sim 10^{-6}$ dyn,[23–25] thermally driven rupture requires a surface tension on the order of 1 dyn/cm.

The problem with the above model is that it precludes the existence of stable pores of finite size. Nevertheless, long-lived pores that remained open for several seconds before resealing have been observed in experiments.[14,16,23–25] Opening of transient pores has been also reported is several computer simulations.[26–29] This has led people to re-examine the basic assumptions underlying Eq. (1). Improved theoretical models succeeded in explaining the formation of stable or long-lived metastable pores by considering the fact that, once pores have been nucleated, their further opening is expected to relax the surface tension.[24,28,30–34] In the case of a planar membrane, it is the increase of the area density of the lipids (occurring concurrently to the dilation of the pore) that reduces the mechanical tension. For vesicles, the opening of

[a)]Current address: Department of Physics and Astronomy, University of Pennsylvania, Philadelphia, Pennsylvania 19104.

a pore allows the internal contents to escape, which reduces the osmotic pressure and the associated Laplace tension.

Most of the theoretical models have so far, however, neglected the effect of membrane fluctuations on the opening and thermodynamic stability of pores. The entropy associated with the shape of the pore has mostly been ignored also. A few recent studies of the entropic contribution to the free energy of nucleating a pore, have led to some new interesting predictions. The most remarkable result has been obtained by Shillcock and Boal[35] in computer simulations of two-dimensional fluid tethered surfaces. They found that pores appeared at zero, and even small negative surface tension. Their interpretation of this surprising finding was that entropy, which favors the formation of noncircular pores, reduces the effective line tension of the pore and makes it negative at sufficiently high temperature. An entirely different fluctuation effect has been discussed by Sens and Safran[36] who considered circular pores, but allowed membrane fluctuations. Their study suggests that positive stress must be applied in order to facilitate the opening of a pore in a fluctuating membrane, and that the nucleation barrier for pore formation is too high to be overcome by thermal fluctuations. More recently, we[37] have demonstrated that the primary effect of membrane fluctuations on circular holes is to reduce the effective surface tension, thereby making the opening of a pore more difficult in comparison to the zero-temperature case.

In this paper, we carry out a statistical mechanical analysis of pore formation in bilayer membranes. Membrane elasticity is described by the Helfrich Hamiltonian, which includes the curvature energy and a surface tension term. A line tension term is introduced to account for the energetic penalty at the pore edge. We calculate the free energy for nucleating a single pore, systematically taking into account both membrane fluctuations and the entropy due to pore shape. We show that, for large enough pores, the pore nucleation free energy takes the form of Eq. (1), with the surface and line tensions replaced by their effective (renormalized) values, $\sigma_{\rm eff}$ and $\Gamma_{\rm eff}$. The effective coefficients are usually smaller than the bare counterparts and, at high enough temperatures, may even be negative. When $\Gamma_{\rm eff}<0$, the opening of a stable pore becomes entropically favored and may occur in weakly stressed membranes. The size of a thermal pore can be varied by changing the tension applied on the membrane.

The paper is organized as follows: The system Hamiltonian is constructed in Sec. II. We show that Eq. (1) for the energy should be augmented by terms representing corrections due to the pore's shape and membrane's height fluctuations. Tracing over the relevant variables yields the corresponding free energy. The derivation of the free energy is presented in Secs. III and IV, in which the thermal corrections to the surface and line tensions are calculated. In Sec. V we discuss our results and suggest some possible further extensions of the present study.

II. DERIVATION OF THE HAMILTONIAN

We consider a bilayer membrane consisting of N lipids that spans a planar circular frame of total area $A_p=\pi L_p^2$, in which a quasicircular pore has been formed. For a nearly flat membrane with arbitrary parametrization $\mathbf{X}(x1,x2)$, the Helfrich Hamiltonian is given by

$$\mathcal{H}=\int_M dx_1 dx_2 \sqrt{g}\left[\sigma+\frac{\kappa}{2}H^2+\overline{\kappa}K\right], \tag{4}$$

where g is the determinant of the metric tensor $g_{\alpha\beta}=\partial_\alpha \mathbf{X}\cdot\partial_\beta \mathbf{X}$, while H and K denote the total and Gaussian curvatures, respectively. The elastic coefficients appearing in the Helfrich Hamiltonian are the surface tension σ, the bending rigidity κ, and the Gaussian rigidity $\overline{\kappa}$. We assume that the bilayer membrane is symmetric with no spontaneous curvature. The integration in Eq. (4) is carried over the two-dimensional manifold M, representing the surface of the membrane.

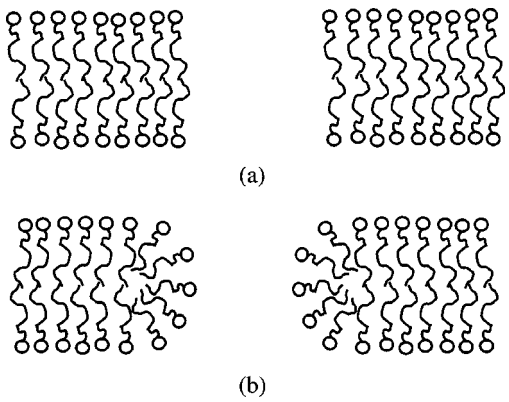

FIG. 1. Schematic microscopic models for hydrophobic (a) and hydrophilic (b) pores. For a hydrophilic pore, the boundary actually joins the two monolayers of the lipid membrane.

A. Gaussian curvature

Understanding the contribution of the Gaussian curvature term [last term in Eq. (4)] to the free energy requires looking at the structure of the membrane on the molecular level. Two distinct models of pores have been discussed in the literature and are shown schematically in Fig. 1. Figure 1(a) depicts a cylindrical pore where the lipids in the vicinity of the pore remain oriented parallel to the membrane surface. Such a pore is called ''hydrophobic,'' and the origin of the pore line tension is the energy due to the exposure of the tails of the lipids at pore's rim to water. The other case is of a ''hydrophilic'' pore, shown in Fig. 1(b), where the lipids curve at the pore's rim thus shielding their hydrophobic parts from the aqueous contact. The line tension of a hydrophilic pore is due to the curvature energy involved in the reorientation of end molecules.

The Gaussian curvature term in the Helfrich Hamiltonian is calculated differently for hydrophobic and hydrophilic pores. For hydrophobic pores, this term reduces to an integral of the geodesic curvature on the pore boundary.[38] A similar situation is encountered in the case of proteins and other membrane inclusions, where the orientation of the lipids at the membrane-inclusion boundary is determined by the structure of the protein.[37] The change in the Gaussian curvature in that case is

$$\Delta\mathcal{H}_{\text{gauss}} = 2\pi\overline{\kappa}(\cos\Omega - 1), \tag{5}$$

where Ω is the contact angle along the boundary.

The case of a hydrophilic pore, on the other hand, is more subtle. Each of the two monolayers making up a bilayer can have an associated Helfrich energy, and the two monolayers are joined at the pore boundary. This, however, does not present a topological boundary and, therefore, there is no integral of the geodesic curvature. The opening of a hydrophilic pore results in a contribution to the Hamiltonian due to the change in topology: The bilayer is topologically a sphere (if we assume both bilayers are linked at the outer radius L_p), which changes genus upon the opening of a pore, becoming a torus. For a manifold without boundary, the Gauss–Bonnet theorem ensures that the total Gaussian curvature is a topological invariant and thus measures, to some extent, the global properties of the membrane. The change in Gaussian curvature energy due to the formation of a hydrophilic pore is given by

$$\Delta\mathcal{H}_{\text{gauss}} = -4\pi\overline{\kappa}. \tag{6}$$

The Gaussian curvature modulus may take both positive or negative values, hence leading to either an increase ($\overline{\kappa}<0$) or decrease ($\overline{\kappa}>0$) in the energy upon the opening of a pore. Strict comparison with classical nucleation theory [Eq. (1)] is possible only for $\overline{\kappa}=0$ and, therefore, we will restrict the following discussion to this special case. The Gaussian curvature term can be interpreted as an additional contribution that lowers or raises the free energy depending on the sign of $\overline{\kappa}$. This contribution is independent of the pore size. It will influence the probability of opening a small nucleation pore, but will have no effect on the size to which metastable long-lived pores grow.

B. Membrane fluctuation energy

The first two terms of the Helfrich Hamiltonian (4) are local in character. Therefore, the above argument regarding the absence of boundaries in a porous membrane fails, and the pore can be treated as if representing the inner membrane boundary. In order to study the statistical mechanical behavior of the membrane, we define a coordinate system $(r,\theta) = (r_0 \leqslant r \leqslant L_p, 0 \leqslant \theta < 2\pi)$ in which the pore is described by a curve of constant $r = r_0$,

$$\mathbf{X}(r,\theta) = [r\cos(\theta) + \eta_x(r,\theta)]\hat{x} + [r\sin(\theta) + \eta_y(r,\theta)]\hat{y} + h(r,\theta)\hat{z}. \tag{7}$$

The function $h(r,\theta)$ represents the height of the membrane above some flat reference plane. The function $r\cos(\theta)\hat{x} + r\sin(\theta)\hat{y} + \boldsymbol{\eta}(r,\theta)$ is a mapping from coordinates (r,θ) in which the membrane pore will be circular, to points in three-dimensional space in which the pores will have an arbitrary shape (see Fig. 2). Thus, $\boldsymbol{\eta}(r_0,\theta)$ is a measure of the deviation of the pore from having a circular projected area, which we will assume to be small. Our choice or r_0, which we will *define* as the radius of the quasicircular pore, is made by equating the projected area of the pore to πr_0^2. More specifically, we will require that $\boldsymbol{\eta}$ satisfies the following boundary conditions (BCs):

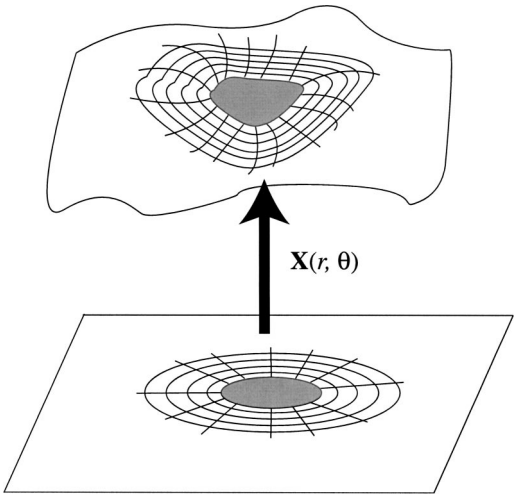

FIG. 2. The mapping $\mathbf{X}(r,\theta)$ takes a flat reference plane containing a circular pore into a curved nearly flat membrane with a hole of nearly circular projected area.

$$\hat{\theta}\cdot\boldsymbol{\eta}(r_0,\theta) = 0, \tag{8}$$

$$\int_0^{2\pi} d\theta[r_0 + \hat{r}\cdot\boldsymbol{\eta}(r_0,\theta)]^2 = \pi r_0^2. \tag{9}$$

On the outer (frame) boundary we set

$$\boldsymbol{\eta}(L_p,\theta) = 0. \tag{10}$$

With the embedding defined by Eq. (7) we have, keeping terms up to quadratic order in $\boldsymbol{\eta}$ and h,

$$\begin{aligned} g_{rr} &= 1 + 2\hat{r}\cdot\partial_r\boldsymbol{\eta} + (\partial_r\boldsymbol{\eta})^2 + (\partial_r h)^2, \\ g_{r\theta} &= \hat{r}\cdot\partial_\theta\boldsymbol{\eta} + r\hat{\theta}\cdot\partial_r\boldsymbol{\eta} + \partial_r h\partial_\theta h + \partial_r\boldsymbol{\eta}\cdot\partial_\theta\boldsymbol{\eta}, \\ g_{\theta\theta} &= r^2 + 2r\hat{\theta}\cdot\partial_\theta\boldsymbol{\eta} + (\partial_\theta\boldsymbol{\eta})^2 + (\partial_\theta h)^2, \end{aligned} \tag{11}$$

for the metric, thus giving us after a lengthy but straightforward calculation

$$\sqrt{g} \approx r[1 + \tfrac{1}{2}(\boldsymbol{\nabla}h)^2 + \boldsymbol{\nabla}\cdot\boldsymbol{\eta} + \boldsymbol{\nabla}\cdot\boldsymbol{\eta}_2], \tag{12}$$

where

$$\boldsymbol{\eta}_2 = (\eta_x\partial_\theta\eta_y)(\hat{r}/r) - (\eta_x\partial_r\eta_y)\hat{\theta}. \tag{13}$$

One also finds that to lowest order the total curvature is given by

$$H = \frac{1}{\sqrt{g}}\partial_\alpha(\sqrt{g}g^{\alpha\beta}\partial_\beta\mathbf{X}) \approx \hat{z}\nabla^2 h + \mathcal{O}(h^2,\boldsymbol{\eta}^2). \tag{14}$$

Substituting Eqs. (12) and (14) into Eq. (4) and keeping terms up to quadratic order in $\boldsymbol{\eta}$ and h, we find

$$\mathcal{H} = \sigma\pi(L_p^2 - r_0^2) + \frac{1}{2}\int dr\,d\theta\,r[\sigma(\nabla h)^2 + \kappa(\nabla^2 h)^2] + \int dr\,d\theta\,r\sigma[\boldsymbol{\nabla}\cdot\boldsymbol{\eta} + \boldsymbol{\nabla}\cdot\boldsymbol{\eta}_2]. \tag{15}$$

The last integral in the above Hamiltonian can be converted into a line integral by the application of the divergence theorem. Using Eqs. (8), (10), and (13) we arrive, after some calculation, to the following form:

$$\mathcal{H}=\sigma\pi(L_p^2-r_0^2)+\frac{1}{2}\int drd\theta r[\sigma(\nabla h)^2+\kappa(\nabla^2 h)^2] - \frac{\sigma}{2}\int_0^{2\pi} d\theta[\hat{r}\cdot\eta(r_0,\theta)]^2-\sigma r_0\int_0^{2\pi} d\theta\hat{r}\cdot\eta(r_0,\theta). \tag{16}$$

An important feature of Eq. (16) is that, *to quadratic order*, the dependence of the Hamiltonian on $h(r,\theta)$ and $\boldsymbol{\eta}(r,\theta)$ decouples completely. Also, notice that Eq. (16) depends only on the boundary value of $\boldsymbol{\eta}$. This is a consequence of the fact that away from the boundary, $\boldsymbol{\eta}$ is merely a transformation of coordinates under which the Helfrich Hamiltonian should be invariant. We will henceforth use the scalar function $\eta(\theta)$ to denote the boundary values of the mapping $\boldsymbol{\eta}(r,\theta)$, i.e., $\eta(\theta)\equiv\hat{r}\cdot\boldsymbol{\eta}(r_0,\theta)$. Using BC (9) of $\eta(\theta)$, we find out that the last two terms of Eq. (16) cancel each other. This leaves us with $\mathcal{H}=\sigma\pi(L_p^2-r_0^2)+\mathcal{H}_h$, where

$$\mathcal{H}_h\equiv\frac{1}{2}\int drd\theta r[\sigma(\nabla h)^2+\kappa(\nabla^2 h)^2]. \tag{17}$$

The Laplacian in the height-dependent Hamiltonian (17) requires that we have two BCs on each boundary. On the outer boundary ($r=L_p$) we impose the BCs,

$$h(L_p)=0 \quad \text{and} \quad \nabla^2 h(L_p)=0. \tag{18}$$

The first BC corresponds to a membrane which is attached to a static frame on its external perimeter. The second is obtained by considering the discrete version of the Helfrich surface Hamiltonian and requiring that in the continuum limit, the same equation describes the motion of the boundary and bulk elements. The BCs on the inner boundary ($r=r_0$) are quite similar,

$$h(r_0,\theta)=H(\theta) \quad \text{and} \quad \nabla^2 h(r_0)=0, \tag{19}$$

with the only difference that the height is set to $H(\theta)$ rather than vanishes. The vector

$$\mathbf{Y}(\theta)\equiv\mathbf{X}(r_0,\theta)=[r_0+\eta(\theta)]\hat{r}+H(\theta)\hat{z}, \tag{20}$$

depicts the locus of the pore boundary in the 3D embedding space. Note that in the case of a membrane inclusion of radius r_0, the second BC in Eq. (19) should be replaced by $-\hat{n}\cdot\nabla h(r_0,\theta)=\partial h(r_0,\theta)/\partial r=H'(\theta)$ where the contact slope, H', depends on the geometry and the tilt angle of the inclusion.[37]

We proceed by writing the height function as $h=h_0+f$, where h_0 is the extremum of Hamiltonian (17), i.e.,

$$-\sigma\nabla^2 h_0+\kappa\nabla^4 h_0=0, \tag{21}$$

subject to the BCs that

$$h_0(L_p)=0, \quad \nabla^2 h_0(L_p)=0, \quad h_0(r_0,\theta)=H(\theta), \quad \nabla^2 h_0(r_0)=0. \tag{22}$$

Equations (19) and (22) imply that the function f, which depicts the fluctuations around the equilibrium profile h_0 satisfies

$$f(L_p)=0, \quad \nabla^2 f(L_p)=0, \quad f(r_0)=0, \quad \nabla^2 f(r_0)=0. \tag{23}$$

Hamiltonian (17) can be thus written as

$$\mathcal{H}_h(h_0+f)=\int drd\theta r\left\{\frac{1}{2}[\sigma(\nabla h_0)^2+\kappa(\nabla^2 h_0)^2] +[\sigma\nabla h_0\cdot\nabla f+\kappa\nabla^2 h_0\nabla^2 f] +\frac{1}{2}[\sigma(\nabla f)^2+\kappa(\nabla^2 f)^2]\right\}. \tag{24}$$

For the cross term (second term in $\mathcal{H}_h$) we obtain, upon integration by parts,

$$\int drd\theta r[\sigma\nabla h_0\cdot\nabla f+\kappa\nabla^2 h_0\nabla^2 f] =\int drd\theta r[-\sigma\nabla^2 h_0+\kappa\nabla^4 h_0]f +\int_{\partial M}\kappa\nabla^2 h_0(\hat{n}\cdot\nabla)f+\int_{\partial M}(\hat{n}\cdot\nabla)[\sigma h_0-\kappa\nabla^2 h_0]f, \tag{25}$$

where the last two integrals in the above equation are performed on the boundaries of the system. The boundary terms in Eq. (25) vanish due to the BCs (22) and (23), while the bulk term vanishes due to Eq. (21).

Without the cross term in Eq. (24), the height-dependent Hamiltonian takes the simple form $\mathcal{H}_h(h_0+f)=\mathcal{H}_h(h_0)+\mathcal{H}_h(f)$, where the energies associated with h_0 (the equilibrium term) and f (fluctuation term) completely decouple. Integrating both terms by parts twice, we find expressions similar to Eq. (25), where h_0 is replaced by f (in the fluctuation term) or vice versa (equilibrium term). In the former, the boundary terms vanish due to Eq. (23) and we are left with

$$\mathcal{H}_h(f)=\int drd\theta r\frac{1}{2}[\sigma(\nabla f)^2+\kappa(\nabla^2 f)^2]. \tag{26}$$

In the latter, the bulk term is eliminated by virtue of Eq. (21). Considering the BCs on h_0 (22), one can easily find that

$$\mathcal{H}_h(h_0)=\frac{1}{2}\int_0^{2\pi} d\theta r_0 H(\theta)\left.\frac{\partial(\kappa\nabla^2 h_0-\sigma h_0)}{\partial r}\right|_{r_0}. \tag{27}$$

In a manner similar to the last two terms in Eq. (16), the last result demonstrates that contributions to the Hamiltonian due to the pore can only appear through boundary (line) integrals.

C. Pore line tension

An additional contribution to the free energy is due to the line tension of the pore, which arises from the curvature and packing of the lipid molecules at the pore boundary (Fig. 1). The pore's shape is depicted by the curve $\mathbf{Y}(\theta)$ (20), and the line tension energy is given by

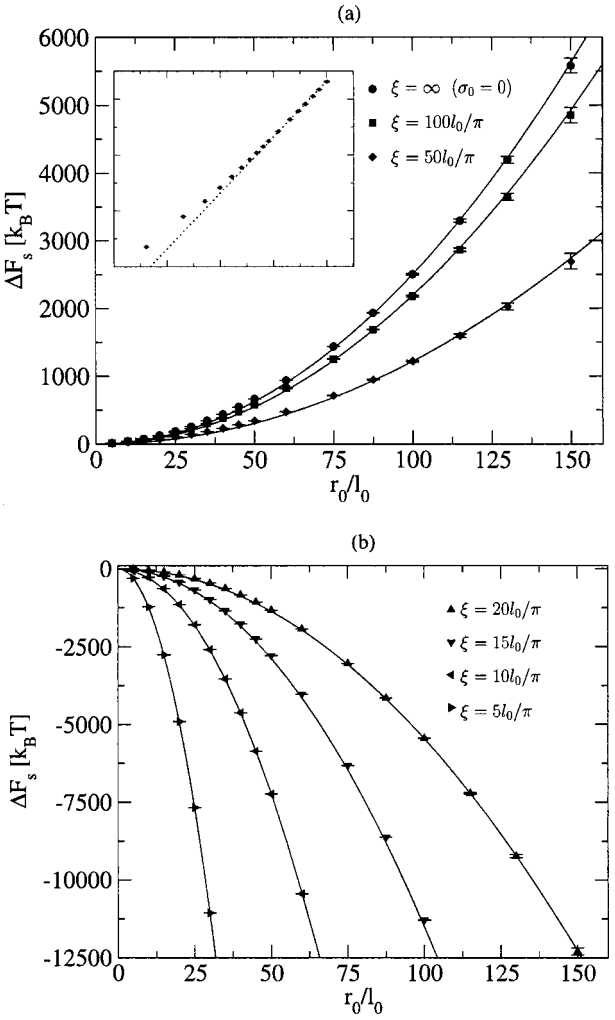

FIG. 3. The free energy ΔF_s as a function of the pore's radius for $\kappa = 10 k_B T$ and various values of σ_0. The inset to graph (a): a log–log plot of the numerical results for $\sigma_0 = 0$. The slope of the straight dotted line is 2.

$$\Gamma \int_0^{2\pi} d\theta \sqrt{(d\mathbf{Y}(\theta)/d\theta)^2}$$

$$\simeq \Gamma 2\pi r_0 + \Gamma \int_0^{2\pi} d\theta \eta(\theta) + \frac{\Gamma}{2r_0} \int_0^{2\pi} d\theta [(dH(\theta)/d\theta)^2 + (d\eta(\theta)/d\theta)^2], \tag{28}$$

where Γ is the line tension coefficient, i.e., the edge energy per unit length.

D. The full Hamiltonian

Collecting expressions (16), (26), (27), and (28), we find that the Helfrich Hamiltonian (excluding the Gaussian curvature term) can be written as the sum of two terms:

$$\mathcal{H} = \mathcal{H}_s + \mathcal{H}_l. \tag{29}$$

The first term is the surface Hamiltonian associated with the membrane fluctuations:

$$\mathcal{H}_s = \sigma\pi(L_p^2 - r_0^2) + \frac{1}{2}\int dr d\theta r[\sigma(\nabla f)^2 + \kappa(\nabla^2 f)^2]. \tag{30}$$

The second is the inner boundary term, consisting of the various contributions to the energy due to the pore

$$\mathcal{H}_l = \Gamma 2\pi r_0 + \frac{1}{2}\int_0^{2\pi} d\theta \left\{ \left[2\Gamma\eta(\theta) + \frac{\Gamma}{r_0}\left(\frac{d\eta(\theta)}{d\theta}\right)^2 \right] + \left[\frac{\Gamma}{r_0}\left(\frac{dH(\theta)}{d\theta}\right)^2 + r_0 H(\theta) \left.\frac{\partial(\kappa\nabla^2 h_0 - \sigma h_0)}{\partial r}\right|_{r_0} \right] \right\}. \tag{31}$$

III. SURFACE TENSION

In calculating the contribution of the surface Hamiltonian (30) to the free energy, we follow the procedure described in our previous manuscript on membrane inclusions.[37] We fix $H(\theta)$ and $\eta(\theta)$ and integrate over the membrane fluctuations f first. We will integrate over the remaining fields in Sec. IV. The integration over the field f is performed by expanding in a series of eigenfunctions $f_{m,n}(r)$ of the operator $\mathcal{L} \equiv -\sigma\nabla^2 + \kappa\nabla^4$: $f(r,\phi) = \Sigma_{m,n} \mathcal{A}_{m,n} f_{m,n}(r) e^{im\phi}$. The functions $f_{m,n}(r)$ can be written as the linear combination of the Bessel functions, $J_m(r)$ and $Y_m(r)$, of the first and second kinds of order m, and the modified Bessel functions of the first and second kinds of order m, $K_m(r)$ and $I_m(r)$:

$$f_{m,n}(r) = AJ_m(\lambda_1^{m,n} r) + BY_m(\lambda_1^{m,n} r) + CK_m(\lambda_2^{m,n} r) + DI_m(\lambda_2^{m,n} r), \tag{32}$$

where the λ_i $(i = 1,2)$ are the positive solutions of $(-1)^{i+1}\sigma(\lambda_i^{m,n})^2 + \kappa(\lambda_i^{m,n})^4 = \mu_{m,n}$, and $\mu_{m,n}$ is the eigenvalue corresponding to the function $f_{m,n}(r)$: $\mathcal{L} f_{m,n}(r) = \mu_{m,n} f_{m,n}(r)$.

Applying the BCs (23) at r_0 and L_p, we derive the eigenvalue equation

$$J_m(\lambda_1^{m,n} r_0) Y_m(\lambda_1^{m,n} L_p) - J_m(\lambda_1^{m,n} L_p) Y_m(\lambda_1^{m,n} r_0) = 0. \tag{33}$$

Although this eigenvalue equation is different from the one we had in Ref. 37, the asymptotic behavior of the eigenvalues is the same. In the long wavelength limit, $\lambda_1^{m,n} r_0 \ll |m|$, Eq. (33) reduces to the eigenvalue equation in the absence of pores

$$J_m(\lambda_1^{m,n} L_p) = 0. \tag{34}$$

This is a manifestation of the fact that modes with characteristic lengths much larger than the pore radius are hardly perturbed by its presence. In the opposite limit, $\lambda_1^{m,n} r_0 \gg |m|$, we find that the difference between two consecutive eigenvalues saturates to $\lambda_1^{m,n+1} - \lambda_1^{m,n} = \pi/(L_p - r_0)$, which is a factor $L_p/(L_p - r_0)$ larger than in the case with no pore. The physical interpretation of this result is that the pore acts like a hard wall for modes with characteristic lengths much smaller than its radius, reducing the effective linear size of the membrane for these modes to $L_p - r_0$.

Integrating over the membrane fluctuations f, the Gibbs free energy is given by[36]

$$G(\sigma,A_p,r_0)=\sigma\pi(L_p^2-r_0^2)+\mathcal{H}_l + \frac{k_BT}{2}\sum_{m,n}\ln\left\{\frac{[\sigma(\lambda_1^{m,n})^2+\kappa(\lambda_1^{m,n})^4]A_p\lambda_{\mathrm{dB}}^2}{2\pi k_BTN}\right\}, \tag{35}$$

where λ_{dB} is the thermal de-Broglie wavelength of the lipids. The Helmholtz free energy is given by $F(A,A_p,r_0)=G-\sigma A$, where the total membrane area A is related to the surface tension by

$$A=\pi(L_p^2-r_0^2)-\frac{1}{2}\int_0^{2\pi}d\theta r_0H(\theta)\left.\frac{\partial h_0}{\partial r}\right|_{r_0} + \frac{k_BT}{2}\sum_{m,n}\frac{1}{\sigma+\kappa(\lambda_1^{m,n})^2}. \tag{36}$$

Assuming that the membrane is incompressible and, therefore, that its total area is fixed, we can use Eq. (36) to derive the following equation, relating the surface tension and r_0:

$$-\pi r_0^2-\frac{1}{2}\int_0^{2\pi}d\theta r_0H(\theta)\left.\frac{\partial h_0}{\partial r}\right|_{r_0}+\frac{k_BT}{2}\sum_{m,n}\left[\frac{1}{\sigma+\kappa(\lambda_1^{m,n})^2} - \frac{1}{\sigma_0+\kappa(\lambda_{1,(0)}^{m,n})^2}\right]=0. \tag{37}$$

In the above equation $\lambda_{1,(0)}^{m,n}$ are the corresponding solutions of the eigenvalue equation in the absence of the inclusion ($r_0=0$): $J_m(\lambda_{1,(0)}^{m,n}L_p)=0$, and $\sigma_0\equiv\sigma(r_0=0)$. The first two terms on the left-hand side of Eq. (37) give the *change* ΔA_0 in the equilibrium area, i.e., the difference between the area of the surface whose profile is parametrized by h_0 and $A_p=\pi L_p^2$, the equilibrium area of the nonporous membrane. The second two terms give the *change* in the area stored in the fluctuations around the equilibrium profile. These changes cancel each other due to the conservation of the *total* area. Since we assume a finite size pore in the thermodynamic limit ($r_0\ll L_p$) and since $H(\theta)\ll L_p$ and $|\partial h_0/\partial r|\ll 1$ (which is why we keep only terms up to quadratic order in h_0), $\Delta A_0\ll A_p$. In this limit, we can expand σ around σ_0, and need only consider terms linear in $\Delta A_0/A_p$:

$$\sigma=\sigma_0(1+\delta),\quad \text{where}\quad \delta\sim\mathcal{O}(\Delta A_0/A_p). \tag{38}$$

After some straightforward algebra we find that the pore free energy, defined as $\Delta F(r_0,h_0,\eta)\equiv F(r_0,h_0,\eta)-F(0,0,0)$, can be expressed by the following sum:[37]

$$\Delta F(r_0,h_0,\eta) =\mathcal{H}_l(\sigma\to\sigma_0,h_0,\eta)-\pi\sigma_0r_0^2 + \frac{k_BT}{2}\sum_{m,n}\ln\left[\frac{\sigma_0(\lambda_1^{m,n})^2+\kappa(\lambda_1^{m,n})^4}{\sigma_0(\lambda_{1,(0)}^{m,n})^2+\kappa(\lambda_{1,(0)}^{m,n})^4}\frac{L_p^2-r_0^2}{L_p^2}\right] \equiv\mathcal{H}_l(\sigma\to\sigma_0,h_0,\eta)+\Delta F_s(r_0), \tag{39}$$

where the sum runs over the modes $n=0,1,...,\sqrt{N_0}$, and, $m=-\sqrt{N_0},\ldots,\sqrt{N_0}$ so that the total number of modes $2N_0$ is proportional to the number of molecules forming the membrane N, while $\lambda_{1,(0)}^{m,n}$ are the corresponding solutions of the eigenvalue equation in the absence of pores (34). Note that despite the implicit coupling between membrane and pore fluctuations (the fields f and h_0, respectively), introduced by Eq. (37), we were able to express the free energy as a sum of: (1) a free energy associated only with the membrane fluctuations ΔF_s, and (2) the Hamiltonian $\mathcal{H}_l$ which depends only on the boundary values $h_0(\theta)$ and $\eta(\theta)$. This can be done only in the thermodynamic limit and for nearly-flat membranes, where terms higher than linear in δ can be neglected in Eq. (38).

An analytical approximation of ΔF_s is obtained by assuming (based on our discussion of the asymptotic behavior of the eigenvalues $\lambda_1^{m,n}$) that eigenvalues such that $\lambda_1^{m,n}r_0<\alpha|m|$ (long wavelength) are not affected by the pore, whereas modes with $\lambda_1^{m,n}r_0>\alpha|m|$ (short wavelength) grow by a factor $L_p/(L_p-r_0)$.[37] The dimensionless constant α is of the order of unity and its value will be determined later by exact numerical calculation of ΔF_s. Using this "step-function" approximation for the eigenvalues $\lambda_1^{m,n}$, and evaluating the sum in Eq. (39) as an integral, we obtain the simple result (correct up to quadratic order in r_0) that

$$\Delta F_s=-\pi r_0^2\sigma_0+\frac{k_BTr_0^2}{\alpha l_0^2}\left\{2-\alpha-\left(\frac{l_0}{\pi\xi}\right)^2\ln\left[\left(\frac{\pi\xi}{l_0}\right)^2+1\right]\right\} \equiv-\pi r_0^2(\sigma_0+\Delta\sigma)\equiv-\pi r_0^2\sigma_{\mathrm{eff}}, \tag{40}$$

where $\xi\equiv\sqrt{\kappa/\sigma_0}$, and $l_0=L_p/\sqrt{N_0}$ is a microscopic length cutoff which is of the order of the bilayer thickness. From the above equation, we identify the thermal correction to the surface tension as

$$\Delta\sigma=\frac{k_BT}{\pi\alpha l_0^2}\left\{\alpha-2+\left(\frac{l_0}{\pi\xi}\right)^2\ln\left[\left(\frac{\pi\xi}{l_0}\right)^2+1\right]\right\}. \tag{41}$$

In order to test the accuracy of expression (40), we have numerically solved the eigenvalue equation (33) and used the solutions to evaluate the sum in Eq. (39). Numerical values of $\Delta F_s(r_0)$ (for $\kappa=10k_BT$ and various values of σ_0) are shown in Figs. 3(a)–3(b). They have been extracted by extrapolating the numerical results obtained for several values of $750\leqslant N_0\leqslant 2000$ to the thermodynamic limit $N_0\to\infty$. In the inset to Fig. 3(a), the results for $\sigma_0=0$ are replotted on a logarithmic scale, showing that our prediction of a quadratic relation between ΔF_s and r_0 is attained only for large (macroscopic) pores with $r_0\gtrsim 100l_0$ (the slope of the straight dotted line is 2). The discrepancy between the numerical values of ΔF_s and Eq. (40) in the small r_0 regime is due to the significant contribution to the free energy of the crossover modes $\lambda_1^{m,n}r_0\sim 1$ which is poorly calculated by the "step function" approximation. The solid curves in Figs. 3(a)–3(b) depict our analytical expression (40) for ΔF_s, with α determined by fitting the results for large r_0 to Eq. (40). The value of α shows a slight dependence on the surface tension varying from 1.60 for $\sigma_0=0$ to 1.75 for $\xi=\sqrt{\kappa/\sigma_0}=5l_0/\pi$.

Our numerical and analytical results suggest that $\Delta\sigma<0$, making the effective surface tension smaller than the bare surface tension. Of particular interest is the fact, demonstrated in Fig. 3(a), that for weakly stretched membranes (large ξ) the effective tension may be negative. In such a case the effective surface tension would act to prevent, rather than

facilitate, the opening of a pore. For strongly stretched membranes (small ξ) the dominant contribution to $\sigma_{\rm eff}$ is of the bare surface tension. In this regime, the surface tension part of the free energy is well approximated by the second term of Eq. (1), i.e., $\Delta F_s \simeq -\sigma_0 \pi r_0^2 \simeq -\sigma \pi r_0^2$.

IV. LINE TENSION

In order to complete the calculation of the free energy, we now need to trace over the fields η and h_0 which in Hamiltonian (31) [see also Eq. (39)] are decoupled from each other. Introducing the Fourier transform of the field η,

$$\eta(\theta) = \frac{d_{\rm dB}}{\sqrt{2N_1}} \sum_{m=-N_1}^{N_1} \tilde{\eta}_m e^{im\theta}, \tag{42}$$

where $d_{\rm dB}$ is the de-Broglie thermal wavelength. Making the particular choice of $\tilde{\eta}_0$ that satisfies the BC (9),

$$\tilde{\eta}_0 \simeq -\frac{d_{\rm dB}}{\sqrt{2N_1}} \sum_{m\neq 0} \frac{|\tilde{\eta}_m|^2}{2r_0}, \tag{43}$$

the corresponding Hamiltonian takes the form

$$\mathcal{H}_l^{\eta} = \frac{\pi d_{\rm dB}^2}{2N_1} \sum_{\substack{m=-N_1 \\ m\neq 0}}^{N_1} |\tilde{\eta}_m|^2 \frac{\Gamma}{r_0}(m^2-1). \tag{44}$$

The $|m|=1$ modes are trivial translation modes which do not contribute to the energy of the pore. The number of $m \geqslant 2$ modes is equal to the number of microscopic degrees of freedom, namely the number of molecules on the rim of the pore. Since this number is proportional to the perimeter of the pore, we can write

$$N_1 \simeq b\left(\frac{r_0}{l_0}\right), \tag{45}$$

where b is a numerical factor of the order of unity. Tracing over the variables $\tilde{\eta}_m$ is straightforward, giving the free energy

$$F_l^{\eta} = \frac{k_B T}{2} \sum_{|m|>1} \ln\left[\frac{d_{\rm dB}^2(m^2-1)\Gamma/r_0}{k_B T N_1}\right]. \tag{46}$$

If the number of modes is large $N_1 \gg 1$ (i.e., $l_0 \ll r_0$) then the sum in the above expression can evaluated as an integral, giving

$$F_l^{\eta} \simeq 2\pi r_0 \frac{b k_B T}{\pi l_0}\left[\frac{1}{2}\ln\left(\frac{b d_{\rm dB}^2 \Gamma}{k_B T l_0}\right) - 1\right]. \tag{47}$$

The contribution of the field h_0 to the line tension free energy is also tractable. From the partial differential equation (21) and the BCs (22), it is easy to show that (for $\sigma_0 > 0$) h_0 can be written by the following mode representation

$$h_0(r,\theta) = \frac{d_{\rm dB}}{\sqrt{2N_1}} \sum_{m=-N_1}^{N_1} \tilde{h}_m \left(\frac{r_0}{r}\right)^{|m|} e^{im\theta} + \tilde{h}_0 \frac{\ln(r/r_0)}{\ln(r_0/L_p)}. \tag{48}$$

Notice that $\nabla^2 h_0 = 0$ everywhere and not only at the boundaries. Substituting expression (48) in Eq. (31), one arrives at the following Hamiltonian:

$$\mathcal{H}_l^h = \frac{\pi d_{\rm dB}^2}{2N_1} \sum_{m=-N_1}^{N_1} |\tilde{h}_m|^2 \left(\frac{\Gamma}{r_0} m^2 + \sigma_0 |m|\right). \tag{49}$$

Assuming that $\sigma_0 \ll \Gamma/r_0$ (the weak stretching regime), it is easy to conclude that the resulting contribution to the free energy $F_l^h \simeq F_l^{\eta}$, and thus

$$\begin{aligned} F_l &= 2\pi r_0 \Gamma + F_l^{\eta} + F_l^h \\ &\simeq 2\pi r_0 \left\{\Gamma + \frac{b k_B T}{\pi l_0}\left[\ln\left(\frac{b d_{\rm dB}^2 \Gamma}{k_B T l_0}\right) - 2\right]\right\} \\ &\equiv 2\pi r_0 (\Gamma + \Delta\Gamma) \equiv 2\pi r_0 \Gamma_{\rm eff}. \end{aligned} \tag{50}$$

We thus identify the thermal correction to the line tension of the pore

$$\Delta\Gamma = \frac{b k_B T}{\pi l_0}\left[\ln\left(\frac{b d_{\rm dB}^2 \Gamma}{k_B T l_0}\right) - 2\right]. \tag{51}$$

For phospholipid bilayers at room temperature $\Delta\Gamma$ is negative and is typically in the range of 10^{-7}–10^{-6} dyn.

V. DISCUSSION AND SUMMARY

The opening of a membrane pore has been traditionally regarded as an energetically-driven process. According to this view, the surface and line tensions are the forces driving, respectively, the opening and closure of pores. The balance between these opposing forces creates a nucleation barrier for the formation of long-lived pores, and requires the opening of a sufficiently large hole at the initial stage.

In previous studies, the role of thermal fluctuations has been limited to facilitating the opening of a nucleation pore. The critical pore size (2) and the height of the barrier (3) have been determined from Eq. (1) for the pore energy. However, at nonzero temperature an entropic part must be added to Eq. (1). To fill the gap in the literature on the subject, we have calculated the thermal contributions to the pore free energy associated with (a) the shape of the boundary of the hole, and (b) the fluctuation spectrum of the membrane. Our study suggests that the pore free energy may be expressed by an equation similar to (1)

$$F = \Gamma_{\rm eff} 2\pi r_0 - \sigma_{\rm eff} \pi r_0^2, \tag{52}$$

in which the bare surface and line tensions are replaced by effective (renormalized) values. Typically, we find that $\Gamma_{\rm eff} < \Gamma$ and $\sigma_{\rm eff} < \sigma$, reflecting two opposite tendencies. The decrease in the line tension reduces membrane stability against pore formation. It reflects the larger configuration space available to a membrane with a hole present. The decrease in the surface tension, on the other hand, makes the formation of pores harder in comparison to the zero-temperature case. This effect originates from the change in the spectrum of membrane fluctuation occurring upon the opening of the pore and the resulting increase in bending energy.

We can identify a number of different regimes of pore stability. For tense membranes with positive effective line tension, we find the standard regime of classical nucleation theory. From Eq. (52), we can identify the stability criteria for the growth of large pores to be $r_0 > \Gamma_{\rm eff}/\sigma_{\rm eff}$. For membranes with low surface tension, the effective surface tension

will be negative. In this regime, pores will increase the free energy for all radii and one should not expect the formation of pores spontaneously as long as the effective line tension is positive. This regime is quite unlike classical nucleation theory, where a nucleation barrier for pore formation always exists.

In the theory of thermally activated poration, the nucleation rate of critical pores depends strongly on the free energy barrier $\delta F = \pi \Gamma_{\rm eff}/\sigma_{\rm eff}$, as $\exp(-\delta F/k_B T)$. The height of the nucleation barrier decreases as one approaches the temperature at which the effective line tension, $\Gamma_{\rm eff}$ (50), vanishes. Above this temperature the barrier disappears and the formation of pores occurs spontaneously. The growth of the pore will not be stopped as long as the surface tension remains positive. If the rate at which the surface tension is relaxed is too small, the membrane will rupture. However, we have demonstrated in Sec. III that membrane fluctuations renormalize the surface tension, making the *effective* tension negative when the *applied* tension is small. Therefore, we may have a situation where both $\Gamma_{\rm eff}$ and $\sigma_{\rm eff}$ are negative. In such a case, the free energy attains a minimum, not a maximum, for $r_0 = \Gamma_{\rm eff}/\sigma_{\rm eff}$, and a stable pore of that radius will be spontaneously formed. The radius of such a pore can be easily varied by several orders of magnitude by varying the applied tension and thereby tuning the value of $\sigma_{\rm eff}$.

The pore size can be also varied by manipulating the magnitude of the line tension, e.g., by the addition of colipids that modify the ability of the lipids to pack at the edge region. Experiments in bilayer lipids to which lysoPC and cholesterol were added demonstrated that these molecules affect the line tension in opposite ways, with the former decreasing the line tension[39] and the latter increasing it.[23,25] Typical values of the line tension found experimentally are in the range of our estimate of the thermal correction $\Delta\Gamma$ or somewhat larger. This demonstrates the significance of thermal effects in determining the stability of membranes against pore formation. In membranes composed of diblock copolymers these effects will probably be weaker since the bare line tension is expected to increase with the membrane thickness while the thermal correction is expected to decrease [see Eq. (51), where the membrane thickness enters as a short-distance cut-off]. Re-examining previous studies which do not include temperature-dependent corrections is of particular importance because the experimental determination of the line tension $\Gamma_{\rm eff}$ is not direct. It is based on a suitable model relating the line tension to other measurable quantities such as the surface tension, pore radius, etc.

To better understand the effect of thermal fluctuations on pore formation, it is necessary to go beyond the second order expansion of the Helfrich Hamiltonian in h and η. In the $\Gamma_{\rm eff} < 0$ regime, the system gains free energy by having pores with large perimeter, which means that holes with shapes that strongly deviate from circular will be highly favorable.[35] By restricting our analysis to small values of the field η (and hence to quasicircular pores only), we probably underestimate the magnitude of the thermal correction to the line tension. Moreover, for negative values of the effective line tension the formation of many pores is also likely to occur, as has been shown in some computer simulations.[40] The collective behavior of these pores and the (membrane-mediated) interactions between them[41] are not well understood. The effect of solvent and in-plane viscosity, which may strongly influence the late-stage dynamical evolution of metastable pores, has been neglected in the present model and should be discussed.[31] More insight on the pores' architecture and their evolution can be gained by molecular-level studies and computer simulations.

ACKNOWLEDGMENTS

We would like to thank P. Pincus, P. Sens, and K. Katsov for stimulating and useful discussions. This work was supported by the NSF under Award No. DMR-0203755. The MRL at UCSB is supported by NSF No. DMR-0080034.

[1] B. Alberts, D. Bray, J. Lewis, M. Raff, K. Roberts, and J. D. Watson, *Molecular Biology of the Cell* (Garland, New York, 1989).
[2] D. S. Dimitrov and R. K. Jain, Biochim. Biophys. Acta **779**, 437 (1984), and references therein.
[3] L. Chernomordik, Chem. Phys. Lipids **81**, 203 (1996).
[4] M. Marsh and H. T. McMahon, Science **285**, 215 (1999).
[5] A. Schmidt, M. Wolde, C. Thiele, W. Fest, H. Kratzin, A. V. Podtelejnikov, W. Witke, W. B. Huttner, and H.-D. Söling, Nature (London) **401**, 133 (1999).
[6] B. Bechinger, Biochim. Biophys. Acta **1462**, 157 (1999).
[7] T. Allen, Curr. Opin. Colloid Interface Sci. **1**, 645 (1996).
[8] R. G. Crystal, Science **270**, 404 (1995); P. L. Felgner, Sci. Am. **276**, 102 (1997).
[9] *Structure and Dynamics of Membranes*, edited by R. Lipowsky and E. Sackmann (Elsevier, Amsterdam, 1995).
[10] I. G. Abidor, V. B. Arakelyan, L. V. Chernomodik, Y. A. Chizmadzhev, V. F. Patushenko, and M. R. Tarasevich, Bioelectrochem. Bioenerg. **6**, 37 (1979).
[11] D. Needham and R. M. Hochmuth, Biophys. J. **55**, 1001 (1989).
[12] C. Wilhelm, M. Winterhalter, U. Zimmermann, and R. Benz, Biophys. J. **64**, 121 (1993).
[13] M. Winterhalter, Colloids Surf., A **149**, 161 (1999).
[14] H. Bermudez, H. Aranda-Espinoza, D. A. Hammer, and D. E. Discher, Europhys. Lett. **64**, 550 (2003).
[15] R. Bar-Ziv, T. Frisch, and E. Moses, Phys. Rev. Lett. **75**, 3481 (1995).
[16] O. Sandre, L. Moreaux, and F. Brochard-Wyart, Proc. Natl. Acad. Sci. U.S.A. **96**, 10591 (1999).
[17] K. Olbrich, W. Rawicz, D. Needham, and E. Evans, Biophys. J. **79**, 321 (2000).
[18] M. A. Guedeau-Boudeville, L. Jullien, and J. M. di Miglio, Proc. Natl. Acad. Sci. U.S.A. **92**, 9590 (1995).
[19] R. Singhvi, A. Kumar, G. P. Lopez, G. N. Stephanopoulos, D. I. C. Wang, G. M. Whitesides, and D. E. Ingber, Science **264**, 696 (1994).
[20] A. Ertel, A. G. Marangoni, J. Marsh, F. R. Hallett, and J. M. Wood, Biophys. J. **64**, 426 (1993).
[21] B. L.-S. Mui, P. R. Cullis, E. A. Evans, and T. D. Madden, Biophys. J. **64**, 443 (1993).
[22] J. D. Litster, Phys. Lett. A **53**, 193 (1975).
[23] D. V. Zhelev and D. Needham, Biochim. Biophys. Acta **1147**, 89 (1993).
[24] J. D. Moroz and P. Nelson, Biophys. J. **72**, 2211 (1997).
[25] E. Karatekin, O. Sandre, and F. Brochard-Wyart, Polym. Int. **52**, 486 (2003).
[26] M. Müller and M. Schick, J. Chem. Phys. **105**, 8282 (1996).
[27] R. D. Groot and K. L. Rabone, Biophys. J. **81**, 725 (2001).
[28] O. Farago, J. Chem. Phys. **119**, 596 (2003).
[29] J. Stecki, J. Chem. Phys. **120**, 3508 (2004).
[30] R. R. Netz and M. Schick, Phys. Rev. E **53**, 3875 (1996).
[31] F. Brochard-Wyart, P. G. de Gennes, and O. Sandre, Physica A **278**, 32 (2000).
[32] V. Talanquer and D. W. Oxtoby, J. Chem. Phys. **118**, 872 (2003).
[33] L. Fournier and B. Joós, Phys. Rev. E **67**, 051908 (2003).
[34] Y. Levin and M. A. Idiart, Physica A **331**, 571 (2004).

[35] J. C. Shillcock and D. H. Boal, Biophys. J. **71**, 317 (1996).
[36] P. Sens and S. A. Safran, Europhys. Lett. **43**, 95 (1998).
[37] C. D. Santangelo and O. Farago, preprint (cond-mat/0309683).
[38] R. D. Kamien, Rev. Mod. Phys. **74**, 953 (2002).
[39] L. V. Chernomordik, M. M. Kozlov, G. B. Melikyan, I. G. Abidor, V. S. Markin, and Yu. A. Chizmadzhev, Biochim. Biophys. Acta **812**, 643 (1985).
[40] J. C. Shillcock and U. Seifert, Biophys. J. **74**, 317 (1998).
[41] R. Bruinsma and P. Pincus, Curr. Opin. Solid State Mater. Sci. **1**, 401 (1996), and references therein.